Sustainable Chemometric Approach Resolving Ternary Anti-COVID-19 Mixture; Statistically Guided Impurity Profiling Using Comparative Assessment Tools and Molecular Docking

Heidi R Abd El-Hadi , Basma M. Eltanany , Soha R. Abd El Hadi , Omar M El-Abassy , Sami El Deeb *

Posted Date: 28 April 2026

doi: 10.20944/preprints202604.1926.v1

Keywords: anti COVID-19 mixture; docking; impurities; multivariate models; sustainability assessment

 doi:10.20944/preprints202604.1926.v1

Article

Sustainable Chemometric Approach Resolving Ternary Anti-COVID-19 Mixture; Statistically Guided Impurity Profiling Using Comparative Assessment Tools and Molecular Docking

Heidi R Abd El-Hadi [1], Basma M. Eltanany [2], Soha R. Abd El Hadi [1], Omar M El-Abassy [1] and Sami El Deeb [3,*]

[1] Pharmaceutical Chemistry Department, Faculty of Pharmacy, Egyptian Russian University, Badr City, Cairo, 11829, Egypt

[2] Pharmaceutical Analytical Chemistry Department, Faculty of Pharmacy, Cairo University, Kasr El-Aini Street, Cairo 11562, Egypt

[3] Institute of Medicinal and Pharmaceutical Chemistry, Technische Universität Braunschweig, Germany

* Correspondence: s.eldeeb@tu-braunschweig.de

Abstract

This study used chemometric models to measure caffeine (CAF), aspirin (ASP), and paracetamol (PAR) in the presence of three hazardous impurities: salicylic acid (SAL), P-nitrophenol (PNP), and P-chloroacetanilide (PCA). A molecular docking study was used to examine how impurities might inhibit cyclooxygenase-2, highlighting the importance of controlling their levels if present in the dosage form. Four sustainable chemometric models: principal component regression, multivariate curve resolution-alternating least squares, artificial neural networks, and partial least squares, were developed. The quantitative analytical performance of all proposed models was evaluated using the per cent recovery, standard error of prediction, and root mean square error of prediction. The developed models covered the concentration ranges (in µg/mL) of PNP (2.00-6.00), PCA (0.50-0.90), SAL (6.00-14.00), ASP (6.00-14.00), CAF (3.00-19.00), and PAR (2.00-10.00). These models effectively addressed collinearity and spectral overlaps. Seven innovative tools, including the Carbon Footprint Reduction Index, Click Analytical Chemistry Index, Multicolour assessment tool, Analytical Green Star Area, spider chart, green solvent selection tool, and Modified Green Analytical Procedure, were used to calculate the sustainability and whiteness of the developed models.

Keywords: anti COVID-19 mixture; docking; impurities; multivariate models; sustainability assessment

1. Introduction

A chronic neurological illness, migraine, is defined by intense unilateral headaches that recur and are often accompanied by autonomic symptoms such as nausea, vomiting, and photophobia [1]. As a debilitating neurological illness, migraine globally influences over one billion people, accounting for the majority of disabled years under the age of 50 [2].

Medication is necessary for the majority of migraine sufferers to alleviate their severe headaches. It is possible to treat migraines using over-the-counter medicines that include either a single ingredient or a combination of two or more drugs, such as paracetamol, aspirin and caffeine or paracetamol and aspirin. [3] Acute COVID-19 infection was associated with an increased risk of headaches for migraine patients [4]. A painkiller and antipyretic paracetamol (PAR) may be used in palliative care to alleviate symptoms of COVID-19 in accordance with World Health Organization recommendations (Figure 1S) [5]. Acetylsalicylic acid, widely recognized as aspirin (ASP), is a

 doi:10.20944/preprints202604.1926.v1

salicylate compound that swiftly undergoes the process of hydrolysis in the body of humans to elicit its curative properties (Figure 1S). Aspirin's anti-inflammatory properties may alleviate fever and body pains in COVID-19 sufferers. Additionally, ASP is administered to COVID-19 patients as a preventative measure. Caffeine (CAF), a purine alkaloid that stimulates the central nervous system, is recognized as 1,3,7-trimethylxanthine (Figure 1S). It is standard procedure to combine CAF with analgesic and antipyretic drugs due to its capacity to augment their efficacy [5,6].

The British Pharmacopoeia Lists P-nitrophenol (PNP) and P-chloroacetanilide (PCA) among PAR impurities (Figure 1S). The synthesis process or storage deterioration might be the source of these impurities. Methemoglobinemia may be caused by PNP, an impurity "F" for PAR [7]. PAR impurity "J" PCA may cause harm to the kidneys and liver [8]. One of the pharmacopeial impurities and critical degradation products of ASP is salicylic acid (SAL) (Figure 1S). According to reports of toxic symptoms [5], it may damage the stomach membrane, the esophagus, and the ears. Among the molecular modeling methods used to assess the binding of a single tiny molecule to a bigger biological target, such as an enzyme or protein, is docking.

A literature review revealed that electrochemical techniques [9–11], spectrophotometric methods [12–15], and chromatographic methods [16–18] were used to determine PAR, ASP, and CAF in their ternary combination.

To the best of our knowledge, no UV-Chemometric method is now accessible for the analysis of this ternary combination together with its harmful impurities. Analytical methods that provide improved sensitivity and selectivity include electrochemistry and chromatography. However, the increased complexity, higher costs of equipment upkeep, and longer analytical durations of these methodologies set them apart. UV-spectrometry is a fast, cheap, and sensitive analytical tool; however, due to spectrum overlap and a lack of specificity, direct UV-spectrophotometric approaches are not appropriate for evaluating multicomponent medication compositions [6,19]. It is believed that chemometric methods are superior to direct UV-spectrophotometric approaches for evaluating complex combinations. A crucial part of the chemometric method that can detect spectra with a high degree of overlap is the simultaneous presence of many spectral wavelengths, which provides more precise results than univariate spectral analysis [20,21].

The aim of this study is to provide a valid eco-friendly chemometric approach for analyzing PAR, ASP, and CAF quantitatively and qualitatively even when harmful impurities are present. Principal component regression (PCR), partial least squares (PLS) multivariate curve resolution-alternating least squares (MCR-ALS), and artificial neural networks (ANN), were applied and validated. Additionally, the impurities toxicity was aimed to be confirmed using molecular docking. The established models were examined for their environmental friendliness using the Carbon Footprint Reduction Index, Click Analytical Chemistry Index, Multi-color assessment tool, Analytical Green Star Area, spider chart, Green solvent selection tool, and Modified Green Analytical Procedure. This will help valorization of developing a specific green analytical approach with high safety margins and low incidence of undesirable harm or excessive samples pretreatment and manipulation.

2. Experimental

2.1. Tools and Software

The Spectra II manager was used in connection with the JASCO dual beam type V-630 UV-visible spectrophotometer (Tokyo, Japan). A spectral slit width of 2 nm and a scanning rate of 1000 nm/min were used. To execute all chemometric techniques, MATLAB® 8.3.0.532 (R2014a) was utilized (Math Works, United States). The Auto dock vina program was used to conduct docking experiments (https://vina.scripps.edu/) and Discovery studio visualizer v21.1.0.20298.

2.2. Reagents and Chemicals

The Pharmaceutical Industry's Delta Pharm kindly donated PAR (Cairo, Egypt). The supplier of ASP and ethanol was El-Nasr Pharmaceutical Co. in Abu Zaabal, Cairo, Egypt. The source of CAF

 doi:10.20944/preprints202604.1926.v1

was LABORT FINE CHEM (India). Their purity values were 99.45% ± 0.422 for PAR, 99.58% ± 0.947 for ASP and 99.91% ± 0.275 for CAF. Sigma Aldrich (Darmstadt, Germany) gave PNP, PCA, and SAL.2.3. Preparation of standard solutions PAR, ASP, CAF, PNP, PCA, and SAL stock standard solutions were prepared in ethanol at 100.00 µg/mL concentrations. Stock standard solutions of PAR, ASP, CAF, PNP, PCA, and SAL were used to make working standard solutions (10.00 µg/mL). Panadol ®Migraine tablet was purchased from a local pharmacy.

2.4. Analysis of Pharmaceutical Preparations

Ten pills were weighed in a tidy mortar and ground to a fine powder. A portion of the weighted pulverized powder was poured into a 100 mL volumetric flask containing 250 mg PAR, 250 mg ASP, and 65 mg CAF. The flask was filled with 40 mL ethanol. The flask was stirred with an ultrasonic shaker for fifteen minutes. Following the filtering procedure with a Whatman filter, the contents of the flask was diluted using ethanol. A 25 mL volumetric flask was filled with an aliquot of filtrate, which was then diluted to the final volume. After that, 1 mL was moved into a 10-mL volumetric flask and diluted to the desired final volume.

2.5. Methods

2.5.1. Principal Component Regression and Partial Least Squares

Mean-centered data and leave-one-out cross-validation were implemented to adjust the total number of latent variables (LVs) in the calibration models that had been established. To obtain the smallest root mean square calibration error (RMSEC), eight latent variables (LVs) were ideal.

2.5.2. Multivariate Curve Resolution-Alternating Least Squares

Spectral and concentration profiles were subjected to non-negativity restrictions derived from the fast non-negativity constrained least squares algorithm (fnnl) in order to extract optimal features with minimal iterations. When optimizing MCR-ALScalibration, these limits were paramount.

2.5.3. Artificial Neural Networks

The ANN calibration approach was improved through the feed-forward model training procedure. The input layer contained 301 neurones, while the output layer contained 6. Also, We tried to stuff as many neurones as possible into the buried layer.Five neurones were chosen from the buried layer using the purelin-purelin transfer function. Linear processes make heavy use of this function. In addition, the optimal number of epochs is 100.

3. Result and Discussion

Drug synthesis or improper storage can result in the formation of impurities and degradation of products. For example, ASP may contain SAL as an impurity, whereas PAR may break down into PNP and PCA. No chemometric methods have been reported for analyzing this three-component mixture in the presence of toxic impurities, despite the fact that there are numerous spectrophotometric methods for analyzing PAR, ASP, and CAF in formulations. In quality control laboratories, multivariate calibration techniques are frequently employed for both drug testing and impurity identification.

Multivariate data analysis was used in this study to resolve drug spectra that overlapped significantly **(Figure 2S**). Four multivariate techniques (PCR, PLS, MCR-ALS and ANN) were used to study PAR, ASP, and CAF in the presence of impurities. Accurate multivariate calibration necessitated careful experimental design of the calibration set. **Table 1** shows that the samples were prepared using a multilevel multifactor design. The training set consisted of 17 samples, whereas the validation set included 8 samples. Scan spectra at 0.1 nm intervals from 260.0 to 290.0 nm for the best results. A total of 301 data points were used to construct and test the calibration models, which were then applied in predicting unknown samples.

 doi:10.20944/preprints202604.1926.v1

Table 1. Concentrations of PAR, ASP, CAF, PNP, PCA and SAL in the calibration and validation sets for the multivariate calibrations.

Mix No.	PAR	ASP	CAF	PNP	PCA	SAL
1	6.00	10.00	11.00	4.00	0.70	10.00
2	6.00	6.00	3.00	6.00	0.60	14.00
3	2.00	6.00	19.00	3.00	0.90	10.00
4	2.00	14.00	7.00	6.00	0.70	8.00
5	10.00	8.00	19.00	4.00	0.60	8.00
6	4.00	14.00	11.00	3.00	0.60	12.00
7	10.00	10.00	7.00	3.00	0.80	14.00
8	6.00	8.00	7.00	5.00	0.90	12.00
9	4.00	8.00	15.00	6.00	0.80	10.00
10	4.00	12.00	19.00	5.00	0.70	14.00
11	8.00	14.00	15.00	4.00	0.90	14.00
12	10.00	12.00	11.00	6.00	0.90	6.00
13	8.00	10.00	19.00	6.00	0.50	12.00
14	6.00	14.00	19.00	2.00	0.80	6.00
15	10.00	14.00	3.00	5.00	0.50	10.00
16	10.00	6.00	15.00	2.00	0.70	12.00
17	2.00	12.00	3.00	4.00	0.80	12.00
18	8.00	6.00	11.00	5.00	0.80	8.00
19	2.00	10.00	15.00	5.00	0.60	6.00
20	6.00	12.00	15.00	3.00	0.50	8.00
21	8.00	12.00	7.00	2.00	0.60	10.00
22	8.00	8.00	3.00	3.00	0.70	6.00
23	4.00	6.00	7.00	4.00	0.50	6.00
24	2.00	8.00	11.00	2.00	0.50	14.00
25	4.00	10.00	3.00	2.00	0.90	8.00

Highlighted rows are concentration of samples in the validation set.

3.1. PCR and PLS Models

PCR and PLS are the two most popular inverse least squares methods for creating multivariate calibration models [22,23]. These models are widely used in spectral analysis to extract meaningful information from large datasets [24]. Both methods take consideration of the relationship between measured responses and concentration levels simultaneously [25]. By removing one sample at a time, the leave-one-out cross-validation approach found the optimum number of components in this research. When using a limited number of components, the optimal number of LVs is the one that minimizes prediction errors. Eight latent factors were found to be the most effective in this instance (Figure 1a,b).

 doi:10.20944/preprints202604.1926.v1

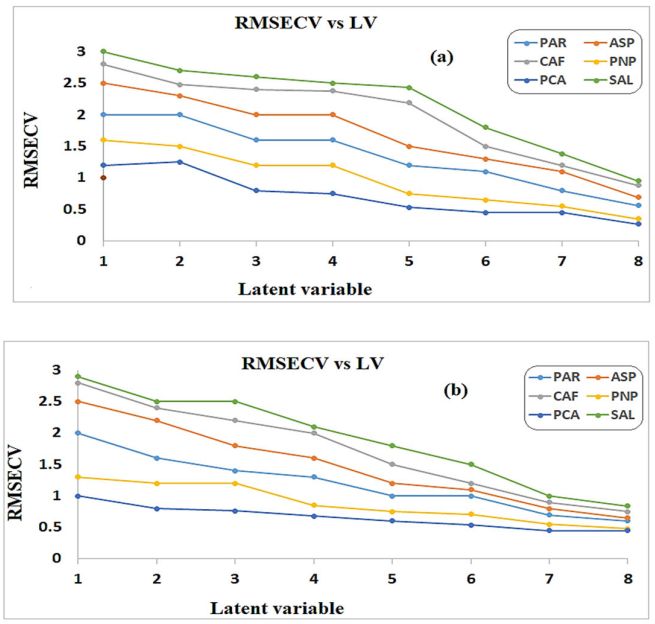

Figure 1. RMSEV plot of the cross-validation results of the calibration set as a function of the number of latent variables used to construct (a) PCR calibration and (b) PLS calibration.

3.2. MCR-ALS Model

The foundation of MCR is factor analysis, which uses a bilinear model and extends Beer's Law over several wavelengths [26,27]. By breaking down the spectral data matrix into distinct concentration and spectral profile matrices for every compound, MCR makes it possible to identify errors [28]. Concentrations from spectral data are iteratively estimated using ALS algorithm, and vice versa. Non-negativity, unimodality, equality, or closure are examples of constraints that can be used to reduce the number of potential solutions during matrix decomposition [29]. The spectral profile matrix was estimated using the "easy-to-use interactive self-modeling analysis" method to start ALS optimization [26].The concentration profile was then determined using this matrix and an unconstrained least-squares method. Both the spectral and concentration profiles in this investigation were subjected to non-negativityconstraints, guaranteeing that all values stayed positive and equal to 6. The ALS algorithm continued until it reached a predetermined 30% convergence threshold. When the change in the root mean square error (RMSE) of the residual matrix "E" between iterations drops below a predetermined threshold, typically 0.1%, convergence usually comes to an end [30]. After ten cycles, iterations continued until the imposed constraints and the convergence condition were both met. High performance indicators, such as the coefficient of determination (R2) of 99.99% and the lack of fit of only 0.158%, validated the efficacy of the approach. Based on the good agreement between the calculated and actual spectra, these results show that the MCR-ALS approach accurately models the spectral profiles **(Figure 2)**. This model was applicable to both qualitative and quantitative analysis.

 doi:10.20944/preprints202604.1926.v1

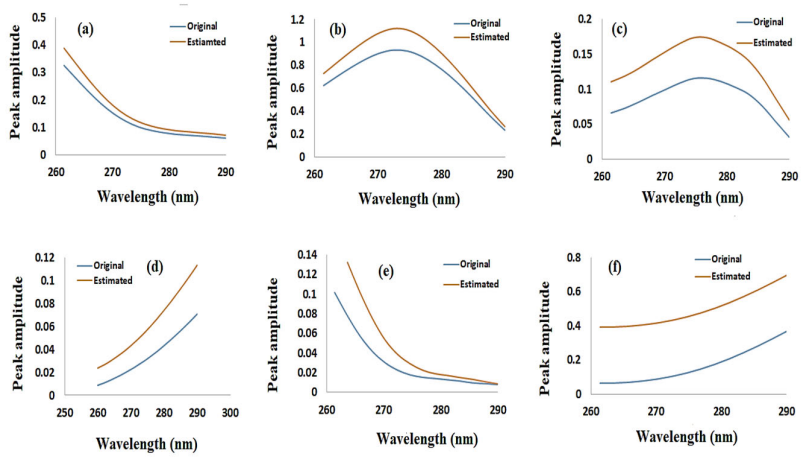

Figure 2. Original spectra and estimated spectra by MCR-ALS of (a) PAR (b) CAF (c) ASP (d) PNP (e) PCA (f) SAL.

3.3. ANN Model

ANNs use a large number of interconnected nodes to determine relationships between inputs and outputs. The input, hidden, and output layers make up a typical ANN [31,32]. A feed-forward ANN model was used in this investigation. The input layer had 301 neurons, corresponding to the number of spectral data points, while the output layer consisted of six neurons, representing the six components under examination. Trial and error were used to determine the optimal number of hidden layer neurons; five neurons worked best when a purelin-purelin transfer function was used and 100 training epochs were run. **(Figure 3)** shows the ANN layout that showed the different layers used for predicting the concentrations of the developed components. Prediction plots for the training, testing, and validation sets are shown in **(Figure 4)**. The model's high predictive power is confirmed by a correlation coefficient (r) near 1 for all sets [22].

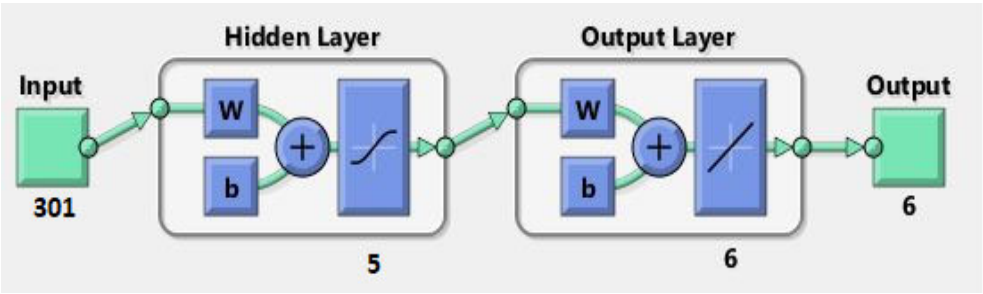

Figure 3. The ANN design uses multiple layers to predicate the concentrations of the studied components.

 doi:10.20944/preprints202604.1926.v1

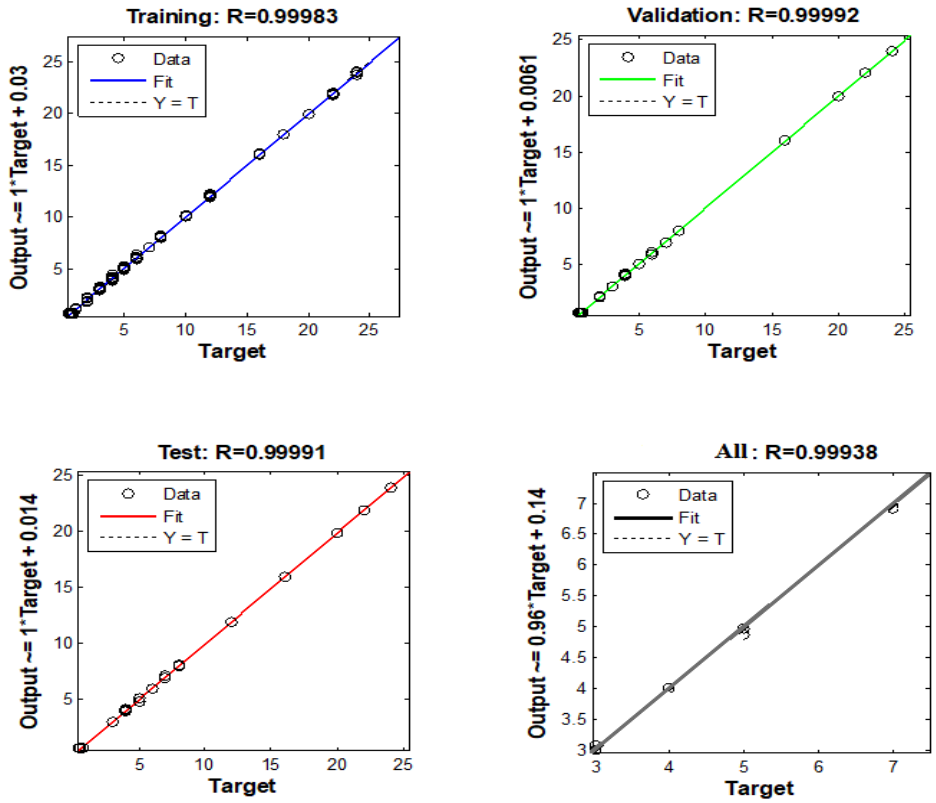

Figure 4. Prediction for the training, test and validation diagrams of ANN model.

Table 2 shows the recovery values, average recoveries, and relative standard deviations (RSD%).The newly created approaches were validated using ICH guidelines [33]. The validation results for the test sets are presented in **(Table 3)**. Furthermore, the models suggested computed the root mean square error of prediction (RMSEP) and root mean square error of calibration (RMSEC) for each component separately.

Column charts for each component illustrate the RMSEP and RMSEC values obtained from the proposed validation and calibration models **(Figure 5)**. Among the methods, ANN showed the lowest RMSEP and RMSEC values. RMSEP serves as a diagnostic tool for assessing prediction errors, reflecting the accuracy and precision of the method. It also indicates variability across concentration ranges and functions similarly to a standard deviation [34]. Based on these results, the ANN method was identified as the most effective model for quantifying individual components.

Table 2. Prediction of validation set samples using the established chemometric models; (a) PCR and PLS,(b) MCR-ALS and ANN.

a) Prediction of validation set samples using PCR and PLS models

Concentration (µg/mL)						PCR						PLS					
PAR	**ASP**	**CAF**	**PNP**	**PCA**	**SAL**	**PAR**	**ASP**	**CAF**	**PNP**	**PCA**	**SAL**	**PAR**	**ASP**	**CAF**	**PNP**	**PCA**	**SAL**
6.00	10.00	11.00	4.00	0.70	10.00	100.58	99.05	98.79	97.45	99.54	102.10	101.03	97.01	98.40	100.7	98.11	98.42
2.00	6.00	19.00	3.00	0.90	10.00	99.01	98.37	99.90	100.76	100.59	98.89	99.11	98.30	98.27	99.54	101.70	99.04
6.00	8.00	7.00	5.00	0.90	12.00	99.12	101.83	98.32	98.88	101.37	101.59	100.53	97.59	100.60	100.41	98.03	97.45
4.00	12.00	19.00	5.00	0.70	14.00	99.88	99.01	98.21	100.24	100.06	101.70	101.08	100.40	97.32	98.81	101.49	98.73
2.00	12.00	3.00	4.00	0.80	12.00	99.30	97.73	99.33	98.64	98.08	101.43	101.39	97.75	98.54	97.74	99.33	101.9
6.00	12.00	15.00	3.00	0.50	8.00	100.24	101.51	98.44	97.30	101.64	101.90	100.43	101.75	100.49	98.89	99.64	101.38
8.00	12.00	7.00	2.00	0.60	10.00	101.25	99.791	99.21	99.93	97.35	101.37	101.25	101.20	98.18	98.80	99.02	99.67
8.00	8.00	3.00	3.00	0.70	6.00	101.92	100.34	98.64	99.34	99.84	102.62	102.24	97.72	99.76	100.78	98.70	99.05
Mean (%)						100.16	99.70	98.85	99.06	99.80	101.45	100.88	98.96	98.94	99.45	99.50	99.45
RSD (%)						1.04	1.45	0.58	1.25	1.49	1.11	0.90	1.85	1.19	1.09	1.40	1.49

b) Prediction of validation set samples using MCR-ALS and ANN models

Concentration (µg/mL)						MCR-ALS						ANN					
PAR	**ASP**	**CAF**	**PNP**	**PCA**	**SAL**	**PAR**	**ASP**	**CAF**	**PNP**	**PCA**	**SAL**	**PAR**	**ASP**	**CAF**	**PNP**	**PCA**	**SAL**
6.00	10.00	11.00	4.00	0.70	10.00	98.05	100.95	98.31	97.50	98.57	99.76	101.12	101.63	101.46	97.90	97.03	99.89
2.00	6.00	19.00	3.00	0.90	10.00	97.53	100.33	100.91	99.46	97.77	98.48	102.69	101.93	99.68	100.53	100.01	98.93
6.00	8.00	7.00	5.00	0.90	12.00	98.47	99.77	98.97	97.62	98.88	98.85	99.45	99.74	98.10	98.88	97.66	98.91
4.00	12.00	19.00	5.00	0.70	14.00	98.13	98.86	100.07	100.30	102.85	98.32	101.53	100.00	99.31	99.44	98.57	98.40
2.00	12.00	3.00	4.00	0.80	12.00	99.55	97.06	101.36	100.11	100.50	99.80	101.48	101.92	98.93	101.10	99.42	97.73
6.00	12.00	15.00	3.00	0.50	8.00	101.88	98.49	98.18	100.47	98.05	98.28	97.79	97.20	101.68	98.90	100.35	98.15
8.00	12.00	7.00	2.00	0.60	10.00	101.71	100.53	97.47	99.18	97.50	101.80	99.02	98.34	98.74	100.52	102.05	97.04

8.00	8.00	3.00	3.00	0.70	6.00	100.25	98.26	102.81	97.53	98.57	98.70	99.21	102.00	100.31	98.54	101.60	100.71
		Mean (%)				99.44	99.28	99.76	99.02	99.08	99.24	100.28	100.34	99.77	99.47	99.58	98.72
		RSD (%)				1.69	1.33	1.84	1.28	1.77	1.19	1.65	1.84	1.28	1.12	1.78	1.17

Table 3. Performance parameters of the calibration and validation sets calculated for each developed model; (a) PCR and PLS,(b) MCR-ALS and ANN.

a) Performance parameters of the calibration and validation sets using PCR and PLS models

Validation parameters	**PCR**						**PLS**					
	PAR	**ASP**	**CAF**	**PNP**	**PCA**	**SAL**	**PAR**	**ASP**	**CAF**	**PNP**	**PCA**	**SAL**
Linearity (μg/mL) [a]	2.00-10.00	6.00-14.00	3.00-19.00	2.00-6.00	0.50-0.90	6.00-14.00	2.00-10.00	6.00-14.00	3.00-19.00	2.00-6.00	0.50-0.90	6.00-14.00
Correlation coefficient (r) [a]	0.9996	0.9998	0.9998	0.9998	0.9997	0.9998	0.9997	0.9998	0.9999	0.9990	0.9993	0.9994
Slope [a]	0.99985	0.98775	1.003383	1.0692	0.9955	1.0066	0.99985	0.98275	0.971667	1.0492	0.9755	0.9966
Intercept [a]	-0.2169	-0.1463	-0.30954	-0.5384	-0.01005	-0.395	-0.1369	-0.0163	-0.067	-0.3584	-0.00205	-0.155
RMSEC [b]	0.124	0.149	0.16	0.151	0.0113	0.18	0.081	0.1095	0.2206	0.1014	0.0109	0.114
RMSEP [c]	0.18	0.21	0.23	0.22	0.01	0.26	0.11	0.15	0.32	0.14	0.01	0.16
LOD [d]	0.32	0.38	0.46	0.12	0.02	0.29	0.26	0.37	0.11	0.34	0.04	0.66
LOQ [d]	0.97	1.15	1.40	0.36	0.08	0.89	0.81	1.14	0.36	1.04	0.14	2.00

b) Performance parameters of the calibration and validation sets using MCR-ALS and ANN models

Validation parameters	**MCR-ALS**						**ANN**					
	PAR	**ASP**	**CAF**	**PNP**	**PCA**	**SAL**	**PAR**	**ASP**	**CAF**	**PNP**	**PCA**	**SAL**
Linearity (μg/mL) [a]	2.00-10.00	6.00-14.00	3.00-19.00	2.00-6.00	0.50-0.90	6.00-14.00	2.00-10.00	6.00-14.00	3.00-19.00	2.00-6.00	0.50-0.90	6.00-14.00

Correlation coefficient (r) [a]	0.999871	0.999976	0.999952	0.999288	0.999232	0.99944	0.999873	0.999877	0.999969	0.999148	0.999272	0.999961
Slope [a]	1.00525	0.98715	0.991374	1.0054	1.02	0.9966	0.98975	0.99715	0.997701	0.99604	1.016	1.0193
Intercept [a]	-0.1249	0.0393	-0.10984	-0.101	-0.024	-0.155	-0.0679	-0.0407	-0.13178	-0.11088	-0.0182	-0.2992
RMSEC [b]	0.06	0.04	0.11	0.05	0.09	0.11	0.07	0.04	0.08	0.07	0.01	0.06
RMSEP [c]	0.09	0.06	0.14	0.07	0.100	0.16	0.11	0.06	0.12	0.11	0.01	0.09
LOD [d]	0.20	0.13	0.22	0.25	0.05	0.66	0.20	0.31	0.18	0.33	0.05	0.17
LOQ [d]	0.61	0.41	0.68	0.92	0.16	2.00	0.60	0.94	0.55	1.01	0.15	0.52

a Data of the straight line plotted between predicted concentrations of each component versus actual concentrations of the calibration set .b Root mean square error of calibration., c Root mean square error of prediction. d LOD and LOQ were calculated from the standard deviation (s) of the response and the slope of the calibration curve (S) according to the following equations: LOD = 3.3(s/S) and LOQ = 10(s/S).

 doi:10.20944/preprints202604.1926.v1

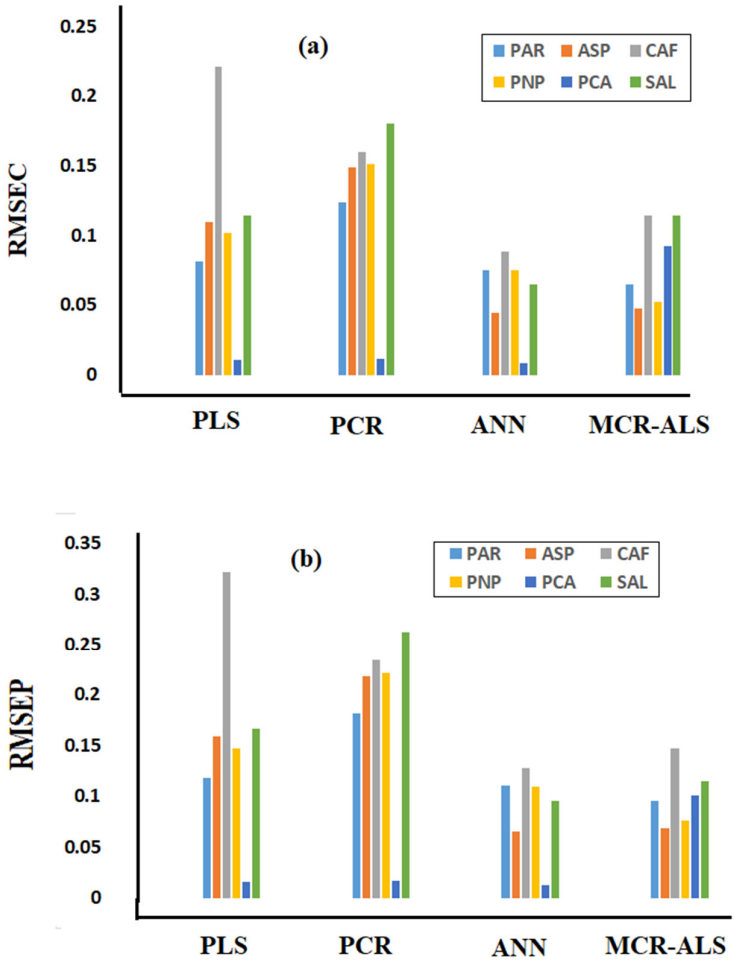

Figure 5. The calculated (a) RMSEC for each component obtained by the proposed validation models and (b) RMSEP obtained by the corresponding calibration model.

3.4. Comparative Statistical Study

This study effectively quantified the PAR and HYO in Panadol® Migraine pills using PCR, PLS, MCR-ALS, and ANN models. A statistical study was carried out to compare the outcomes of the published method with those of a new regression methodology [17]. The t-test and F-ratio tests found strong agreement between the new and published methods, with no significant differences as shown in **(Table 4)**. The reported and established methods were compared using a one-way analysis of variance test (ANOVA) **(Table 5)**. The findings demonstrated that the groups were not significantly different from one another, and the computed F-values were lower than the critical one.

Table 4. Statistical analysis of the results obtained by the established chemometric models and the reported HPLC method for the determination of PAR, ASP and CAF in pharmaceutical dosage form.

Parameters	PAR					ASP					CAF				
	Proposed methods				Reported Method [a]	Proposed methods				Reported Method [a]	Proposed methods				Reported Method [a]
	PCR	PLS	MCR-ALS	ANN	HPLC	PCR	PLS	MCR-ALS	ANN	HPLC	PCR	PLS	MCR-ALS	ANN	HPLC
Mean [b] (%)	100.31	100.00	99.94	100.06	101.56	100.81	100.09	99.93	99.67	100.89	100.42	100.42	101.09	100.62	101.58
SD	1.260	1.529	1.603	1.639	0.906	1.011	1.047	1.121	1.065	1.378	1.289	1.041	0.757	0.871	1.648
Variance	1.58	2.33	2.56	2.68	0.82	1.02	1.09	1.25	1.13	1.89	1.66	1.08	0.57	0.75	2.71
n	6	6	6	6	6	6	6	6	6	6	6	6	6	6	6
Student's t-test (2.23)[c]	1.97	2.16	2.16	1.96	-	0.12	1.14	1.32	1.72	-	1.35	1.45	0.66	1.26	-
F-value c (5.05)[c]	1.93	2.85	3.13	3.27	-	1.86	1.73	1.51	1.67	-	1.63	2.51	4.74	3.58	-

a HPLC method using methanol, glacial acetic acid, and water (28:3:69 v/v) at flow rate of 2ml/min, detection at 275.0 nm [17]. b Average of 6 experiments. c Figures between parentheses represent the corresponding tabulated values of t and f at P= 0.05.

 doi:10.20944/preprints202604.1926.v1

Table 5. One-way ANOVA statistical analysis within 95% confidence interval on the recovery percentage data obtained from application of the chemometric methods and the reported HPLC methods on Panadol® migran tablet.

	Source of variation	SS	df	MS	f	P-value	F-crit
PAR	**Between groups**	4.08	4	1.02	0.54	0.70	2.75
	Within groups	46.88	25	1.87	-	-	-
ASP	**Between groups**	5.25	4	1.31	1.36	0.27	2.75
	Within groups	24.11	25	0.96	-	-	-
CAF	**Between groups**	2.77	4	0.69	0.75	0.56	2.75
	Within groups	22.86	25	0.91	-	-	-

Another method that may be used to find out whether there is a significant difference between the means of distinct groups is Tukey's simultaneous significant difference test [35]. Horizontal lines representing each group's data range are shown in **(Figure 3S)**, with the group mean in the middle. The overlapping intervals show that there was no discernible difference between the mean values derived from the suggested and reported approaches for various pharmaceutical formulations.

The second statistical tool that was employed was the interval plot [35]. With the mean value at the center of each line, it displays confidence intervals as vertical lines. There are no discernible differences between the suggested and reported methods for different pharmaceutical formulations when the plot's intervals for each method overlap **(Figure 4S)**. Another crucial data visualization tool is the boxplot, with the median indicated by a line inside the box and the middle 50% of the data (the interquartile range) represented by the central box. Higher values are indicated by the upper lines, and lower values are indicated by the whiskers [36].

As shown in **Figure 5S**, this figure illustrates the distribution of data within each group.The last statistical technique for determining whether data have a normal distribution is the normal probability plot. If the majority of the points in a pharmaceutical formulation closely match the straight reference line, the data is said to be normally distributed [36]. The results were shown in **(Figure 6S)**.

3.5. Molecular Docking Study

Among the molecular modeling methods used to assess the binding of a single tiny molecule to a bigger biological target, such as an enzyme or protein, is docking. It is crucial to research this kind of molecule-enzyme interaction because tiny molecule binding can alter the natural conformation of the enzyme and ultimately cause it to lose some or all of its activity.

Two fundamental steps underpin molecular docking studies: first, all potential ligand molecule conformations and binding site placement are examined; second, binding energies are investigated using multiple docking score functions to assess each ligand's capacity to bind to a protein. Here, we assess each ligand's binding energies using the London ΔG scoring function. The COX-2 site of activity is a hydrophobic channel that forms an L-shaped channel along the length of the protein. The lobby, a sizable aperture at the channel's mouth, is followed by a constriction consisting of an H-bond network formed by the arrangement of three hydrophilic residues (Arg-120, Tyr-355, and Glu-524). The result of the constriction is a forked channel with a selective side pocket and a major hydrophobic pocket. The crucial catalytic residue Tyr-385, Trp-387, Phe-518, and Ser-530 encircle the main pocket, which stretches far into the active site. The amino acids Val-523, His 90, and Arg-513 define the selectivity pocket, which is situated just above the constriction. In addition to interactions with the primary active site channel, the physically bulkier selective COX-2 inhibitors can fit into the bigger COX-2 selectivity side-pocket because the less sterically hindered amino acid Val 523 is present in COX-2 rather than Ile-523 in COX-1.

 doi:10.20944/preprints202604.1926.v1

The purpose of this study is to evaluate the abilities of the following impurities PCA, PNP and SAL to inhibit the cyclooxygenase enzyme-2 (PDB ID: 6COX).The docking studies demonstrated that PCA, PNP and SAL can attach to the major cleft of COX-2, where critical amino acids (Tyr-385 and Ser-530) are found in COX-2 enzyme's pocket. As shown in (Figure 7S). The carbonyl group of PCA establishes a hydrogen bond with Ser-530 and Tyr-385 amino acid residues which are a portion of the enzyme's primary cleft similar to reported binding modes of potent inhibitors as celecoxib, ASP and PAR [37,38], confirming that PCA may block the enzyme in a comparable manner to paracetamol with binding Score (-8.1 kcal/mol). Also, several hydrophobic interactions with Ala-527 and Val-349. Moreover, both PNP and SAL have a crucial hydrogen bond with Ser-530 and Tyr-385 amino acid residues in COX-2 binding site with binding Scores (-9.9 and 9.1 kcal/mol, respectively). Extra hydrogen bond is formed in PNP with Met-522 to increase fitting in the COX-2 pocket. In addition, hydrophobic interactions with Trp-387 and Leu-352 in PNP, and several hydrophobic interactions with Val-349 and Gly-526 in salicylic acid were formed. The aforementioned interaction has been shown to be responsible for nociception and pyrexia comparable to standard drug as ASP and PAR.

This analysis provides not only the possible mechanism of action but also the docking modes inside the binding pocket of the protein. Based on the results described above, the impurities compounds may be responsible for analgesic and antipyretic activities on the basis of their interactions with targeted proteins.

Despite the COX-2 enzyme's optimal binding mechanism for impurity compounds, these findings have a double-edged effect because of the high toxicity of impurities to human health.

3.6. Evaluation of the Greenness

Evaluating the ecological effects of various analytical methods in light of their conformity to green chemistry principles was crucial, rather than relying only on the authors' assumptions or preferences.

3.6.1. Carbon Footprint Reduction Index (CaFRI)

CaFRI is a specialized tool for evaluating the greenness of analytical laboratory procedures, with a focus on carbon footprint. This instrument assigns a score ranging from 0 to 100 based on a variety of criteria, including energy and chemical consumption, waste management, recycling, and personnel logistics [39]. The outcome is represented by an intuitive footprint diagram, with red, yellow, and green zones indicating poor, average, and favorable performance, respectively. The associated software is freely available online at (https://bit.ly/CaFRI) [40]. A score of 66 is determined by applying CaFRI to evaluate the suggested methods, and the results are shown in **Table 6.**

Table 6. An overview of the greenness assessment.

aFRI	CACI	AGSA	MA tools
		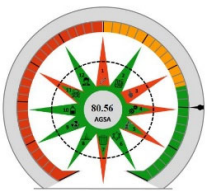	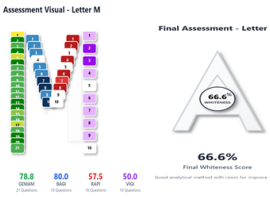

MOGAPI	Hansen space	Primary spider diagram	Secondary chart for health hazards, general

 doi:10.20944/preprints202604.1926.v1

	characteristics, fire safety, and stability
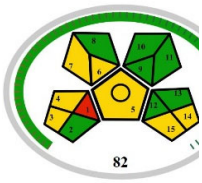 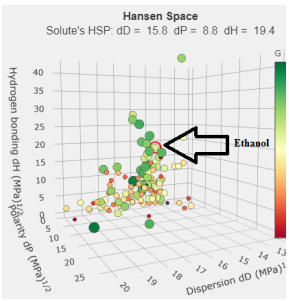  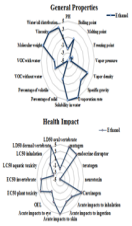 	

3.6.2. The Click Analytical Chemistry Index (CACI)

The Click Analytical Chemistry Index (CACI) program (bit.ly/CACI2025) was utilized to assess the economic value and feasibility of the approach [41,42]. The evaluation included eight criteria: the amount of samples, preparing the samples complexity, practicality, application breadth, mobility, automating level, sensitivity, and analysis time. The CACI evaluation received a score of 75, indicating strong practical application with a focus on implementing accessibility and cost-efficiency **(Table 6)**.

3.6.3. Application of AGSA

The AGSA indicator systematically ranks an analytical method's compliance with the 12 Principles of GAC to give a thorough and structured assessment of its environmental friendliness [43]. The scoring system assesses many aspects of an analytical process. Specific questions with three-tiered answer choices are used to assess each topic, enabling a progressive division of methods. Greater environmental responsibility is implied by higher ratings, which supports techniques that use less energy, treat samples as little as possible, and favor non-hazardous substances. The resulting pictogram is depicted in **Table 6** and has a 80.56 environmentally positive score.

3.6.4. Multi-Color Assessment Tool (MA Tool)

It is a comprehensive online platform established to combine four well-known assessment models into a single, cohesive evaluation system. The MA Tool, which can be found at https://effervescent-naiad-a47bbd.netlify.app/, integrates the Green Evaluation Metric for Analytical Methods (GEMAM), Blueness Assessment Graphical Index (BAGI), Redness Analytical Performance Index (RAPI), and Violet Innovation Grade Index (VIGI) into a structured 51-question assessment protocol [44].

GEMAM is represented by 21 questions that analyze sustainability standards for the environment. The 10-question BAGI assesses operational applicability and practical viability.The RAPI evaluates analytical performance parameters by responding to 10 questions.VIGI is represented by 10 questions that examine the degree of innovation and quality control procedures.

Each segment's color intensity across all indices indicates the score magnitude, providing a quick visual understanding of the outcomes. The composite percentage value is shown at the center of a 3D-styled white capital letter "A" that represents the total Whiteness Score. The combination of the percentage value and the letter "M" creates the "M-A" insignia, which stands for Method Assessment and represents the transition from multidimensional evaluation (M) to a single sustainability representation (A) [44] . The overall MA Whiteness Score, calculated as the average of all four assessment tools, was 66.6%, indicating good Performance **(Table 6)**.

 doi:10.20944/preprints202604.1926.v1

3.6.5. Greenness Evaluation with the Modified Green Analytical Procedure Index

GAPI's fifteen components may be used to test and assess every facet of an analytical process, including sample preparation and volume, solvent and reagent health risks, instruments, waste amount, and handling. Green indicates a modest influence on the natural surroundings, whereas red and yellow indicate a medium and major impact, respectively. While comparing several approaches, the GAPI statistic falls short in providing a complete assessment. The analytical Eco Scale provides a correct total score, and the MoGAPI tool combines it with the visual impact of GAPI [45,46]. The software was used to assess the environmental sustainability of the proposed analytical procedures, as shown in **Table 6**. The aggregate score of 82 suggested a completely eco-friendly technique.

3.6.6. Green Solvent Selection Tool

An amazing study tool, the green solvent selection tool is used by many manufacturing companies to find the best environmentally sustainable greener solvent. A method developed by GlaxoSmithKline (GSK) utilises information from solvent safety data sheets to assess the advantages and disadvantages of various solvents. Table 6 illustrates that many features, including hydrogen bonding, polarity, and dispersion, are used to evaluate solvents on a scale from zero to ten. Additionally, a chemometric equation, represented by G, may be used to determine the most environmentally friendly solvents [47–49].

$$G = \sqrt[4]{(H \times S \times E \times W)} \quad (1)$$

Here, H stands for health, S for safety, E for the environment, and W for waste management. G is the green solvent score. The approach that was strongly suggested required performing calculations on ethanol. The following is an explanation of the formula that produces the values for H, S, E, and W:

(G ethanol=6.6/Hwater= 8.9/ S water= 7.7/ E water=6.7/W water= 4.2)

The findings demonstrate that the solvent, ethanol, has little impact on the environment.

3.6.7. Greenness Index Based on Spider Chart Measurement

The constituents included in the suggested chemometric procedures were evaluated using a spider diagram in order to ascertain their greenness level. Data used in this tool is derived from solvent safety data sheets, which include comprehensive information on a reagent's properties, including its effects on SHE (safety, health, and the environment) throughout the whole process. As shown in **(Table 6)**, a hierarchical spider diagram was created to demonstrate the general environmental sustainability of the required compounds. Five major subcategories are reviewed to arrive at this primary figure. Each group received a score from -5 to +5 after considering the effects on health, overall characteristics, odour, fire safety, and stability. Spider graphics that supplement the main figure and provide further details for each of the five subcategories shown in (Table 6). For the sake of simplicity, we assumed that any information not included in the solvent safety data sheets for the five subcategories listed above was equal to zero. This is because many chemical reagents do not have readily available data [50,51].

5. Conclusions

The present study demonstrated the use of chemometry by demonstrating how it may be employed to concurrently ascertain a ternary combination with its potentially dangerous contaminants utilizing simple methods requiring little adjustment. Four chemometric methods efficiently identify six analytes, assisting quality control labs in resolving six-drugs overlap. In this investigation, six analytes' spectra were estimated using methods that were both accurate and efficient. The most successful method, according to RMSEC and RMSEP, was MCR-ALS. Molecular docking demonstrated that the impurities had analgesic and antipyretic effects, and that prolonged exposure caused harmful side effects. No statistically significant difference was seen between the groups. In conclusion, the suggested methodologies have been effectively used and verified for the

 doi:10.20944/preprints202604.1926.v1

simultaneous determination of PAR, ASP, and CAF in pharmaceutical formulations and pure powders. These results suggest the utility of eco-friendly assessed chemometric models, as potential impurity profiling analyses tools with minimal sample preparation and data manipulation.

Supplementary Materials: The following supporting information can be downloaded at the website of this paper posted on Preprints.org, Figure 1S: Chemical structure of (a)PAR, (b) ASP, (c) CAF (d) PNP, (e) PCA and (f) SAL;Figure 2S: UV-spectra of PAR, ASP, CAF, PNP, PCA and SAL using ethanol as solvent;Figure 3S: Tukey,s simultaneous significant difference test for the developed and published methods of (a) PAR, (b) ASP and (c) CAF in dosage form; Figure 4S: Interval plot for the developed and published methods of (a) PAR, (b) ASP and (c) CAF in dosage form;Figure 5S: Box plot for the developed and published methods of (a) PAR, (b) ASP and (c) CAF in dosage form; Figure 6S: Normal probability plot for the developed and published methods of (a) PAR, (b) ASP and (c) CAF in dosage form;Figure 7S: Docking results for 2D and 3D binding sites of a) PCA, b) PNP and c) SAL with COX-2 enzyme for analgesic and antipyretic activity.

Author Contributions:"Conceptualization,H.R.A.E and O.M.E.; methodology, H.R.A.E and O.M.E.; software, H.R.A.E and S.R.A.E .; validation,H.R.A.E; formal analysis, O.M.E.; investigation, H.R.A.E and O.M.E; resources, H.R.A.E and O.M.E; data curation, H.R.A.E and O.M.E.; writing—original draft preparation,H.R.A.E and O.M.E.; writing—review and editing, B.M.E and S.E.; visualization, H.R.A.E, S.R.A.E and O.M.E..; supervision, B.M.E and S.E; project administration, H.R.A.E, S.R.A.E and O.M.E..; funding acquisition, No fund.

Funding: This research received no external funding.

Informed Consent Statement: Not Applicable.

Data Availability Statement: All data are available from the corresponding author upon request.

Conflicts of Interest: The authors declare no conflict of interest.

Abbreviations

CAF	Caffeine
ASP	Directory of open access journals
PAR	Three letter acronym
SAL	Linear dichroism
PNP	P-nitrophenol
PCA	P-chloroacetanilide
PCR	Principal component regression
MCR-ALS	Multivariate curve resolution-alternating least squares
ANN	Artificial neural networks
PLS	Partial least squares

References

1. Yang, J.; Song, X.; Shi, L.; Zhang, J.; Huang, G.; et al. New insights into the increased risk of migraines from COVID-19 infection and vaccination: A Mendelian randomization study. Front. Neurol 2024, 15, 1445649.
2. Ashina, M.; Buse, D.C.; Ashina, H.; Pozo-Rosich, P.; Peres, M.F.P.; Lee, M.J.; et al. Migraine: Integrated approaches to clinical management and emerging treatments. Lancet 2021, 397, 1505–1518.
3. Diener, H.C.; Gaul, C.; Lehmacher, W.; Weiser, T. Aspirin, paracetamol (acetaminophen) and caffeine for the treatment of acute migraine attacks: A systematic review and meta-analysis of randomized placebo-controlled trials. Eur. J. Neurol 2022, 29, 350–357.
4. Magdy, R.; Elmazny, A.; Soliman, S.H.; Elsebaie, E.H.; Ali, S.H.; Abdel Fattah, A.M.; et al. Post-COVID-19 neuropsychiatric manifestations among COVID-19 survivors suffering from migraine: A case–control study. J. Headache Pain 2022, 23, 101.
5. Marzouk, H.M.; Ibrahim, E.A.; Hegazy, M.A.; Saad, S.S. Sustainable liquid chromatographic determination and purity assessment of a possible add-on triple-action over-the-counter pharmaceutical combination in COVID-19. Microchem. J. 2022, 178, 107400.

 doi:10.20944/preprints202604.1926.v1

6. El-Adl, S.M.; Mattar, A.A.; El-Abassy, O.M.; Sebaiy, M.M. Development of UV-chemometric techniques for resolving the overlapped spectra of aspirin, caffeine and orphenadrine citrate in their combined pharmaceutical dosage form. BMC Chem. 2025, 19, 75.
7. El Sherbiny, D.; Wahba, M.E.K. Analysis of some pharmaceuticals in the presence of their synthetic impurities by applying hybrid micelle liquid chromatography. Open Chem. 2020, 18, 377–390.
8. Farid, J.F.; Mostafa, N.M.; Fayez, Y.M.; Essam, H.M.; ElTanany, B.M. Chemometric quality assessment of paracetamol and phenylephrine hydrochloride with paracetamol impurities; comparative UV-spectrophotometric implementation of four predictive models. Spectrochim. Acta A Mol. Biomol. Spectrosc. 2022, 265, 120308.
9. Yiğit, A.; Yardım, Y.; Çelebi, M.; Levent, A.; Şentürk, Z. Graphene/Nafion composite film modified glassy carbon electrode for simultaneous determination of paracetamol, aspirin and caffeine in pharmaceutical formulations. Talanta 2016, 158, 21–29.
10. Yiğit, A.; Yardım, Y.; Şentürk, Z. Voltammetric sensor based on boron-doped diamond electrode for simultaneous determination of paracetamol, caffeine, and aspirin in pharmaceutical formulations. IEEE Sens. J. 2015, 16, 1674–1680.
11. Sanghavi, B.J.; Srivastava, A.K. Simultaneous voltammetric determination of acetaminophen, aspirin and caffeine using an in situ surfactant-modified multiwalled carbon nanotube paste electrode. Electrochim. Acta 2010, 55, 8638–8648.
12. Hajian, R.; Soltaninezhad, A. The spectrophotometric multicomponent analysis of a ternary mixture of paracetamol, aspirin, and caffeine by the double divisor-ratio spectra derivative method. J. Spectrosc. 2013, 2013, 405210.
13. Moţ, A.C.; Soponar, F.; Medvedovici, A.; Sârbu, C. Simultaneous spectrophotometric determination of aspirin, paracetamol, caffeine, and chlorphenamine from pharmaceutical formulations using multivariate regression methods. Anal. Lett. 2010, 43, 804–813.
14. Özdemir, A.; Dinç, E.; Onur, F. Utilization of multivariate calibration techniques for the spectrophotometric simultaneous determination of paracetamol, aspirin and caffeine in a pharmaceutical formulation. Turk. J. Pharm. Sci. 2004, 1, 139–151.
15. Bouhsain, Z.; Garrigues, S.; de la Guardia, M. PLS-UV spectrophotometric method for the simultaneous determination of paracetamol, acetylsalicylic acid and caffeine in pharmaceutical formulations. Fresenius J. Anal. Chem. 1997, 357, 973–976.
16. Yenda, P.; Katari, N.K.; Ettaboina, S.K.; Satheesh, B.; Muchakayala, S.K.; Gundla, R. An effective and stability-indicating method development and optimization utilizing the Box–Behnken design for the simultaneous determination of acetaminophen, caffeine, and aspirin in tablet formulation. Biomed. Chromatogr. 2023, 37, 55-85.
17. Saeed, A.M.; Mohammed, O.J.; Hussein, N.G. Validation of liquid chromatographic analytical method for determination of aspirin, caffeine and paracetamol in some pharmaceutical tablet forms in Iraqi market. Res. J. Pharm. Technol. 2023, 16, 215–220.
18. Abdel-Halim, L.M.; Ramadan, N.K.; Rahman, M.K.; Galal, M.M. GC and HPTLC-densitometric methods for simultaneous determination of aspirin, paracetamol, caffeine anhydrous, dextromethorphan hydrobromide and chlorpheniramine maleate: Method validation and application to over-the-counter tablets. Bull. Fac. Pharm. Cairo Univ. 2023, 61, 7.
19. Sayed, R.A.; Ibrahim, A.E.; Sharaf, Y.A. Chemometry-assisted UV-spectrophotometric methods for the simultaneous determination of paritaprevir, ritonavir, and ombitasvir in their combined tablet dosage forms: A comparative study. J. Chemom. 2021, 35, 3321.
20. Kelani, K.M.; Hegazy, M.A.; Hassan, A.M.; Tantawy, M.A. Univariate versus multivariate spectrophotometric methods for the simultaneous determination of omarigliptin and two of its degradation products. Spectrochim. Acta A Mol. Biomol. Spectrosc. 2022, 271, 120880.
21. Yehia, A.M.; Elbalkiny, H.T.; Riad, S.M.; Elsaharty, Y.S. Chemometrics for resolving spectral data of cephalosporins and tracing their residue in wastewater samples. Spectrochim. Acta A Mol. Biomol. Spectrosc. 2019, 219, 436–443.

 doi:10.20944/preprints202604.1926.v1

22. Abd El-Hadi, H.R.; Eissa, M.S.; Zaazaa, H.E.; Eltanany, B.M. Development and validation of chemometric-assisted spectrophotometric models for efficient quantitation of a binary mixture of supportive treatments in COVID-19 in the presence of its toxic impurities: A comparative study for eco-friendly assessment. BMC Chem. 2023, 17, 1–16.
23. Dong, J.D.; Zhang, Y.Y.; Wang, Y.S.; Wu, M.L.; Zhang, S.; Cai, C.H. Chemometry use in the evaluation of the Sanya Bay water quality. Braz. J. Oceanogr. 2010, 58, 339–352.
24. Mouhamed, A.A.; Nadim, A.H.; Mostafa, N.M.; Eltanany, B.M. Application of smart chemometric models for spectra resolution and determination of challenging multi-action quaternary mixture: Statistical comparison with greenness assessment. BMC Chem. 2024, 18, 1–14.
25. Wagieh, N.E.; Hegazy, M.A.; Abdelkawy, M.; Abdelaleem, E.A. Quantitative determination of oxybutynin hydrochloride by spectrophotometry, chemometry and HPTLC in presence of its degradation product and additives in different pharmaceutical dosage forms. Talanta. 2010, 80, 2007–2015.
26. Shaaban, H.; Mostafa, A.; Al-Zahrani, B.; Al-Jasser, B.; Al-Ghamdi, R. Simultaneous determination of drugs affecting central nervous system (CNS) in bulk and pharmaceutical formulations using multivariate curve resolution-alternating least squares (MCR-ALS). J. Anal. Methods Chem. 2020, 2020, 1–8.
27. Antunes, M.C.; Simão, J.E.J.; ACD, R.T. Multivariate curve resolution of overlapping voltammetric peaks: Quantitative analysis of binary and quaternary metal mixtures. Analyst. 2002, 127, 809–817.
28. X, A.; Drug, A. Innovative earth-friendly multivariate techniques for quantitative and qualitative analysis of triamterene and xipamide as antihypertensive drug combination. Spectrochim. Acta A Mol. Biomol. Spectrosc. 2024, 285, 121234.
29. El-Ragehy, N.A.; Yehia, A.M.; Hassan, N.Y.; Tantawy, M.A.; Abdelkawy, M. Chemometrics tools in detection and quantitation of the main impurities present in aspirin/dipyridamole extended-release capsules. J. AOAC Int. 2016, 99, 948–956.
30. Abd El-Hadi, H.R; Eissa, M.S.; Zaazaa, H.E.; Eltanany, B.M. Univariate versus multivariate spectrophotometric data analysis of triamterene and xipamide: A quantitative and qualitative greenly profiled comparative study. BMC Chem. 2023, 17, 1–14.
31. Tantawy, M.A.; Michael, A.M. Artificial neural networks versus partial least squares and multivariate resolution-alternating least squares approaches for the assay of ascorbic acid, rutin, and hesperidin in an antioxidant formulation. Spectrosc. Lett. 2019, 52, 1–7.
32. Zeid, A.M.; Abdelazim, A.H.; Shahin, M. Simultaneous spectrophotometric quantitative analysis of elbasvir and grazoprevir using assisted chemometric models. Spectrochim. Acta A Mol. Biomol. Spectrosc. 2021, 252, 119505.
33. ICH, Q1A(R2). Stability testing of new drug substances and products. International Conference on Harmonization, IFPMA, Geneva, Switzerland, 2003.
34. Abd El-Hadi, H.R.; Eissa, M.S.; Zaazaa, H.E.; Eltanany, B.M. Chemometric quality assessment of doxylamine succinate with its degradation product; implementation of two predictive models on UV-spectrophotometric data of anti-emetic binary mixture. J. AOAC Int. 2022, 105, 1–10.
35. Abd El-Hadi, H.R.; Eltanany, B.M.; Zaazaa, H.E. Smart spectrophotometric approaches for estimation of difluprednate in existence of its synthetic precursor and alkaline degradation product; comparative statistical studies and analytical ecological appraisal. Bull. Fac. Pharm. Cairo Univ. 2024, 62, 32–43.
36. Abd El-Hadi, H.R. Comparative statistical evaluation of greenness, blueness, and whiteness spectrophotometric methods for dexamethasone and chloramphenicol estimation. Sci. Rep. 2025, 15, 1–12.
37. Yadav, T.C.; Kumar, N.; Raj, U.; Goel, N.; Vardawaj, P.K.; Prasad, R.; et al. Exploration of interaction mechanism of tyrosol as a potent anti-inflammatory agent. J. Biomol. Struct. Dyn. 2020, 38, 382–397.
38. Jahan, I.; Sakib, S.A.; Alam, N.; Majumder, M.; Sharmin, S.; Reza. Pharmacological insights into Chukrasia velutina bark: Experimental and computer-aided approaches. Anim. Model Exp. Med. 2022, 5, 377–388.
39. Mansour, F.R.; Nowak, P.M. Introducing the carbon footprint reduction index (CaFRI) as a software-supported tool for greener laboratories in chemical analysis. BMC Chem. 2025, 19, 1–12.
40. Bahgat, E.A.; Saleh, H.; Darwish, I.M.; El-Abassy, O.M. Green HPLC technique development for the simultaneous determination of the potential combination of mirabegron and tamsulosin. Sci. Rep. 2025, 15, 1–10.

 doi:10.20944/preprints202604.1926.v1

41. Mansour, F.R.; Bedair, A.; Locatelli, M. Click Analytical Chemistry Index as a novel concept and framework, supported with open source software to assess analytical methods. Adv. Sample Prep. 2025, 14, 100164.
42. Nabil, M.; Ahmed, D.A.; Abbas, S.S.; Lotfy, H.M.; Marzouk, H.M. Green HPLC strategy for quantification of carvedilol and hydrochlorothiazide in cardiac medications with in-vitro dissolution kinetics and impurity profiling. BMC Chem. 2025, 19, 1–10.
43. Mansour, F.R.; Bedair, A.; Belal, F.; Magdy, G.; Locatelli, M. Analytical Green Star Area (AGSA) as a new tool to assess greenness of analytical methods. Sustain. Chem. Pharm. 2025, 46, 102051.
44. Abbas, A.E.F.; Al Kamaly, O.; Magdy, G.; Halim, M.K. MA tool—Multi-color assessment platform for white analytical chemistry: Unified evaluation of method greenness, practicality, performance, and innovation. Microchem. J. 2025, 216, 108512.
45. El-Kafrawy, D.S.; Issa, A.E.; Beltagy, Y.A.; El-Shoubashy, O.H. A challenging multi-purpose HPLC-DAD concurrent determination of sulfacetamide with two pharmacopeial impurities, three co-formulated drugs and interfering preservative in ophthalmic drops: Triad color appraisal of sustainability. Microchem. J. 2025, 114342.
46. Mansour, F.R.; Płotka-Wasylka, J.; Locatelli, M. Modified GAPI (MoGAPI) tool and software for the assessment of method greenness: Case studies and applications. Analytica 2024, 5, 451–457.
47. Hafez, H.M.; Mostafa, A.A.; El-Abassy, O.M. Spider diagram with greenness assessment criteria for mathematical UV spectrophotometric methodologies for separating overlaid spectrum signals of diclofenac sodium and lidocaine hydrochloride. Green Anal. Chem. 2025, 13, 100265.
48. Kayali, Z.; Obaydo, R.H.; Sakur, A.A. Spider diagram and sustainability evaluation of UV-methods strategy for quantification of aspirin and sildenafil citrate in the presence of salicylic acid in their bulk and formulation. Heliyon. 2023, 9, e14612.
49. Larsen, C.; Lundberg, P.; Tang, S.; Ràfols-Ribé, J.; Sandström, A.; Lindh, E.M.; et al. A tool for identifying green solvents for printed electronics. Nat. Commun. 2021, 12, 4510.
50. Lotfy, H.M.; Obaydo, R.H.; Nessim, C.K. Spider chart and whiteness assessment of synergistic spectrophotometric strategy for quantification of triple combination recommended in seasonal influenza—Detection of spurious drug. Sustain. Chem. Pharm. 2023, 32, 100980.
51. Shen, Y.; Lo, C.; Nagaraj, D.R.; Farinato, R.; Essenfeld, A.; Somasundaran, P. Development of Greenness Index as an evaluation tool to assess reagents: Evaluation based on SDS (Safety Data Sheet) information. Miner. Eng. 2016, 94, 1–9.